Torque Ripple and Misalignment Torque Compensation for the Built-In Torque Sensor of Harmonic Drive Systems

Hamid D. Taghirad and P. R. Bélanger

***Abstract*— A harmonic drive is a compact, lightweight, and high-ratio torque transmission device which is used in many electrically actuated robot manipulators. In this paper a built-in torque sensor for harmonic-drive systems is examined in detail. The method proposed by Hashimoto, in which strain gauges are directly mounted on the flexspline, is employed and improved in this paper. To minimize sensing inaccuracy, four Rosette strain gauges are used employing an accurate positioning method. To cancel the torque ripples, the oscillation observed on the measured torque and caused mainly by gear teeth meshing, Kalman filter estimation is used. A simple fourth-order harmonic oscillator proved to accurately model the torque ripples. Moreover, the error model is extended to incorporate any misalignment torque. By on-line implementation of the Kalman filter, it has been shown that this method is a fast and accurate way to filter torque ripples and misalignment torque. Hence, the intelligent built-in torque sensor is a viable and economical way to measure the harmonic-drive transmitted torque and to employ that for torque feedback strategies.**

***Index Terms*—Built-in torque sensor, harmonic drive, Kalman filter, misalignment torque, positioning error, torque ripples, torque sensing.**

I. Introduction

DEVELOPED in 1955 primarily for aerospace applications, harmonic drives are high-ratio and compact torque transmission systems. Every harmonic drive consists of the three components illustrated in Fig. 1. The wave generator is a ball bearing assembly with a rigid, elliptical inner race and a flexible outer race. The flexspline is a thin-walled, flexible cup adorned with small, external gear teeth around its rim. The circular spline is a rigid ring with internal teeth machined along a slightly larger pitch diameter than those of the flexspline. When assembled, the wave generator is nested inside the flexspline, causing the flexible circumference to adopt the elliptical profile of the wave generator and the external teeth of the flexspline to mesh with the internal teeth on the circular spline along the major axis of the wave generator ellipse.

If properly assembled, all three components of the transmission can rotate at different but coupled velocities on the same axis. To use the harmonic drive for speed reduction, the wave generator is mounted on the electric motor shaft, and the output is conveyed either through the circular spline while the flexspline is fixed or through the flexspline while the circular spline is fixed. In the latter case, by rotation of the wave generator, the zone of gear-tooth engagement is carried with the wave generator major elliptical axis. When this engagement zone is propagated 360° around the circumference of the circular spline, the flexspline which contains fewer teeth than the circular spline will lag by that smaller number of teeth relative to the circular spline. Through this gradual and continuous engagement of slightly offset teeth, every rotation of the wave generator moves the flexspline a small angle back on the circular spline, and through this unconventional mechanism, gear ratios up to 320 : 1 can be achieved in a single transmission.

The harmonic drive exhibits performance features both superior and inferior to those of conventional gear transmissions. Its performance advantages include high-torque capacity, concentric geometry, lightweight and compact design, zero backlash, high efficiency, and back drivability. Harmonic drive systems suffer however, from high flexibility, resonance vibration, friction, and structural damping nonlinearities [1]. In numerous robotic control techniques such as feedback linearization, computed torque method, and some adaptive control schemes, the actuator torque is taken to be the control input [2]–[4]. This can only be accomplished through torque feedback at each joint of the robot [5].

In order to apply torque feedback on the robot joint, it is necessary to measure the transmitted torque through the actuator transmission mechanism. Conventionally, torque sensors are placed in the output transmission line of the robot [6], [7]. However, for a harmonic drive transmission, which has an elastic element, the flexspline, there is no advantage to add an additional compliant element and thereby reduce the joint stiffness. In this paper we are using the idea of a built-in torque sensor for harmonic drives as first proposed by Hashimoto in 1989 [8]. This method proved to be an economical and effective way of torque sensing for harmonic drives in our setup, as claimed by Hashimoto *et al.* [9]. In our testing station a Wheatstone bridge of four Rosette strain gauges is utilized to sense the torsional torque transmitted through the flexspline. A practical and accurate method is proposed to mount the strain gauges on the flexspline in order to minimize any radial or circumferential misplacement of each strain gauge.

Manuscript received June 1, 1997; revised April 1, 1998.

The authors are with the Center for Intelligent Machines, Department of Electrical Engineering, McGill University, Montréal, P.Q., H3A 2A7 Canada (e-mail: taghirad@cim.mcgill.ca).

Publisher Item Identifier S 0018-9456(98)05616-2.

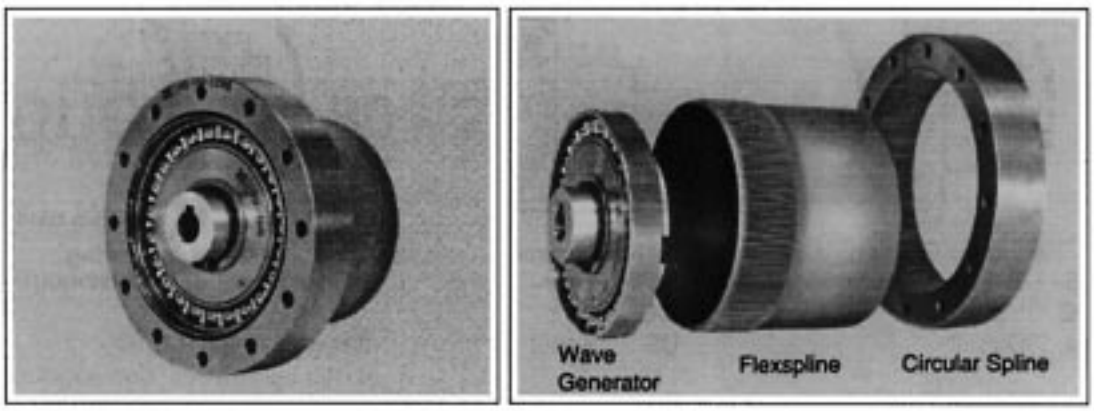

Fig. 1. Harmonic drive components.

One important characteristic of harmonic drive torque transmission, as observed in free motion experiments, is a high frequency oscillation in the output torque signal. These oscillations, named torque ripples, whose principal frequency of oscillation (in rad/s) is twice the motor velocity (in rad/s), are mainly caused by harmonic-drive gear-meshing vibration. A small fraction of the torque ripples are caused by the nonideal torque measurement, because of the direct attachment of strain gauges on the flexspline. Since the flexspline has an elliptical shape, strain gauges mounted on the flexspline are subjected to unwanted strain caused by the elliptical shape. We show in this paper, however, that using four Rosette strain gauges and using an accurate method to mount the strain gauges, will reduce the amplitude of the torque ripple to a minimum. Moreover, the dependence of the frequency content of the torque ripples on the velocity makes it possible to model them as a simple harmonic oscillator and to employ a Kalman filter to predict and filter them from the torque measurement. If only low-frequency torque control is desired [5], the high-frequency ripples may be removed by estimating them via Kalman filtering. This is more efficient than simple low-pass filtering, because it uses the known structure of the torque signal.

A fourth-order harmonic oscillator error model is proposed in this paper to characterize both the fundamental and first-harmonic frequency content of the torque ripple. Using this model for the torque ripples, a prediction-type Kalman filter algorithm is applied to estimate the torque ripples. The performance of the on-line Kalman filter implemented for torque ripple cancellation is shown to be quite fast and accurate.

The Kalman filter is used not only to estimate the torque ripples but also to cancel any mechanical misalignment torque signature on the measured torque. Many torque sensors exhibit the limitation of being sensitive to the torques applied in the direction perpendicular to their axis of measurement. In our setup, after repeated use of the harmonic drive system for different experiments, a similar torque signature was observed in the measured torque. After examining the system accurately, the source of this torque signature is found to be the misalignment of the harmonic drive shaft and the load. The frequency of the misalignment torque (in rad/s), it can be intuitively identified from its source of generation, is found to be exactly the same as the output shaft velocity (in rad/s). Therefore, by adding another block to the harmonic oscillator model we managed to estimate the misalignment component of the measured torque. By using the extended model for the torque ripple and misalignment torque together, it is shown that the filtered torque cancels the torque ripple and misalignment torque quite accurately. The experimental results obtained from combining the original ideas introduced in this paper with a robust torque controller design given in [5] and [10] proves that built-in torque sensors are viable and economical means to measure harmonic drive transmitted torque and to employ them for torque feedback strategies.

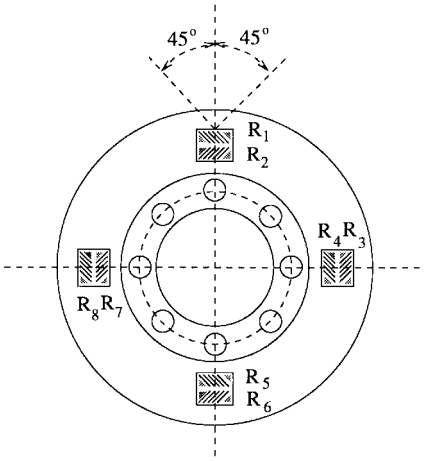

Fig. 2. Position of four Rosette strain gauges on the flexspline diaphragm.

II. Built-In Torque Sensor

As illustrated in Fig. 2, four Rosette strain gauges are mounted on the diaphragm part of the flexspline. A Rosette stain gauge consists of two separate strain gauges perpendicularly mounted on one pad. For a clockwise torque exerted on the flexspline illustrated in Fig. 2, strain gauge R_1 is under compression while strain gauge R_2 is under tension. Similarly, all odd-indexed strain gauges illustrated in Fig. 2 are under compression, while the others are under tension. Thus, a Wheatstone bridge of strain gauges as illustrated in Fig. 3 can transduce the torsion into a difference voltage. The reason

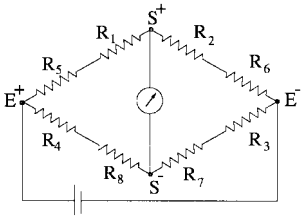

Fig. 3. Strain gauges Wheatstone bridge network.

why Rosette strain gauges are necessary for the harmonic drive built in torque sensor, as explained in [9], is to compensate for the elliptical shape of the flexspline. If the strain caused by applied torque is named ϵ_t, while the strain caused by the elliptical shape of flexspline is called ϵ_w, Hashimoto *et al.* [11] illustrated that the strain applied to strain gauges R_1 and R_2 are

$$\begin{aligned}\epsilon_1 &= \epsilon_t + \epsilon_w \\ \epsilon_2 &= -\epsilon_t + \epsilon_{w'}\end{aligned} \tag{1}$$

where $\epsilon_{w'}$ is assumed in [9] to be a sinusoidal modulation of ϵ_w. Thus,

$$\epsilon_1 - \epsilon_2 = 2\epsilon_t + \Psi_0 \sin(2\beta). \tag{2}$$

In order to cancel the modulation $\Psi_0 \sin(2\beta)$ and to detect the actual torsional strain ϵ_t, the information from strain gauges R_3 and R_4 is necessary. These strain gauges are located at an angle of 90° from strain gauges R_1 and R_2, and therefore

$$\epsilon_3 - \epsilon_4 = 2\epsilon_t + \Psi_0 \sin(2\beta - \pi). \tag{3}$$

Therefore, a Wheatstone bridge, constructed from strain gauges R_1 to R_4 is sufficient to produce a difference voltage proportional to the torsional strain ϵ_t as follows:

$$\begin{aligned}E_{\text{out}} &= \frac{K}{4}(\epsilon_1 + \epsilon_3 - \epsilon_2 - \epsilon_4)E_{\text{sup}} \\ &= K\epsilon_t E_{\text{sup}}\end{aligned} \tag{4}$$

in which K is the gauge factor, and E_{out} and E_{sup} denote output and supply voltages, respectively.

Although only two Rosette strain gauges are sufficient to extract the torsional strain, two other Rosette strain gauges are introduced to maintain symmetry and to minimize the effect of positioning error. Sensing inaccuracies are caused by radial, circumferential, and angular positioning error. Radial positioning error occurs when the gauges are placed on different radii from the center of the flexspline. As shown in Fig. 2, even without any radial displacement of the strain gauges, radial error exists, since strain gauges R_1 and R_2 are placed at different radii. However, by using four Rosette strain gauges, as illustrated in Fig. 2, this error will be compensated by strain gauges R_5 and R_6, which are located in the reverse position.

Circumferential positioning error occurs when two Rosette strain gauges are mounted in an angle different than 90° from each other. This positioning error introduces more sensing inaccuracies than radial positioning error [11], [12]. Angular positioning error occurs when a Rosette strain gauge is not mounted perpendicular to the flexspline's axis of rotation. This

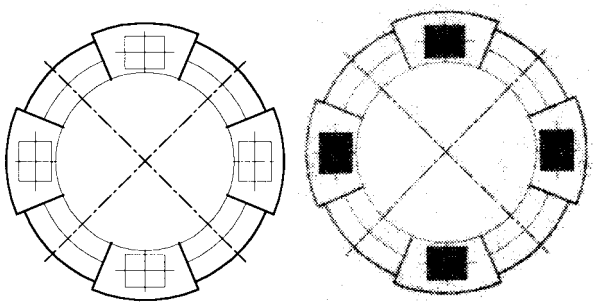

Fig. 4. Proposed transparent film for accurate strain-gauge placement.

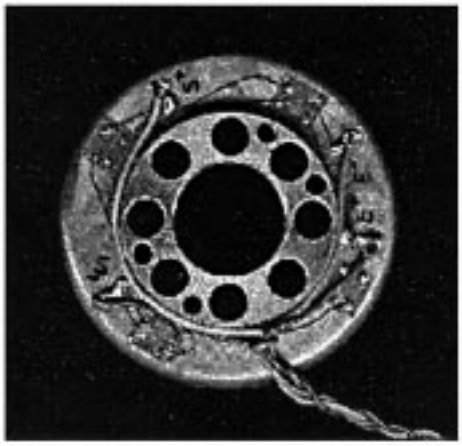

Fig. 5. Harmonic drive built-in torque sensor.

positioning error also introduces sensing inaccuracy similar to the circumferential positioning error. To minimize the positioning error, we propose a method using a specially designed transparent film for the strain gaugs placement. As illustrated in Fig. 4, an accurate drawing of the strain gauge placement positions is printed on a transparent film using a laser printer with the finest possible lines. Then the strain gauges are placed on the transparent film using a microscope. By these means, all positioning errors are reduced to a minimum, and as examined in our testing station to other placement methods, the sensing inaccuracy is minimized. When the strain gauges are mounted on the transparent film as illustrated in Fig. 4, the transparent film is placed on the flexspline and the strain gauges are cemented on the surface. The final configuration of the wired strain gauges is illustrated in Fig. 5. The harmonic drive used in the testing station and illustrated in Fig. 5 is from RHS series of HD systems, with gear ratio of 100 : 1, and rated torque of 40 Nm. The flexspline diameter is 46 mm, and its length is 49 mm. To amplify the output signal, a variable range amplifier with a gain 1000 is used. It generates 10 V dc voltage as input voltage to the Wheatstone bridge.

III. Torque Sensor Calibration

To examine the dynamics of the torque sensor and to calibrate it, we locked the harmonic-drive wave generator and applied a known torque on the flexspline. The locking device is a simple shaft resembling the motor shaft, which can be

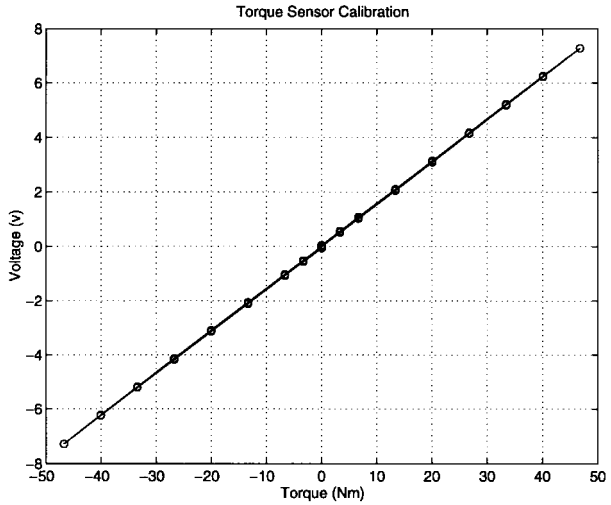

Fig. 6. Torque sensor calibration results for full-range loading.

TABLE I
TORQUE SENSOR CALIBRATION RESULTS

Torque Sensor Gain	Consistency Measure
6.60 Nm/Volts	2%

fixed to the ground. The output torque is applied using arm and weight method. The torque calibration details of loading and unloading some weight on the arm in both directions. This experiment is repeated at different flexspline positions, to check the position dependence of the torque sensor. Also, low-range and full-range loading experiments are tested at each position to evaluate the nonlinearity of the torque sensor. A typical result for the full-range loading experiment is shown in Fig. 6. These data are best fitted by a straight line using least-squares approximation. The estimated torque sensor gain for each experiment is calculated from the slope of this line. However, this gain is deemed acceptable only if it is consistent for other experiments. By consistency we mean a statistical measure, namely *the ratio of the standard deviation to the average value of estimated parameter for different experiments* [1]. If this measure is small, we have a good consistency for different experiments, and the final gain is obtained from the average value of the estimated gain for different experiments. The final gain is obtained by this method for eight experiments, and the results are given in Table I, where the gain is 6.6 Nm/V, with a low consistency measure of 2%. This illustrates that the torque sensor is quite linear, and it is not position dependent. Moreover, the torque sensor gain is consistent for different operating conditions.

IV. TORQUE RIPPLE COMPENSATION

One important characteristic of the harmonic-drive torque transmission, as observed in free motion experiments, is a high frequency oscillation in the output torque signal (see torque curve in Fig. 7). These oscillations, named torque ripples, were also observed by other researchers [13]. Torque ripples are caused mainly by harmonic drive gear meshing vibration. Harmonic drive gear meshing vibration introduces a real torque oscillation which can be observed in the end effector motions of robots using harmonic drives and even sensed by hand when back-driving the harmonic drive. Its principal frequency of oscillation (in rad/s) is twice the motor velocity (in rad/s), for the gear teeth in harmonic drives are meshing in two zones. A small fraction of the torque ripples are caused by the nonideal torque measurement, because of the direct attachment of strain gauges on the flexspline. Since the flexspline has an elliptical shape, strain gauges mounted on the flexspline are subjected to unwanted strain caused by the elliptical shape. Hashimoto [9] proposed using at least two pairs of Rosette strain gauges to compensate for this unwanted strain. However, ideal compensation is possible only if there is no positioning error of strain gauges. As explained in Section II, it has been shown, however, that using four Rosette strain gauges, and using an accurate method to mount the strain gauges, will reduce the amplitude of the torque ripple to a minimum. Unfortunately, the frequency of torque ripples (in rad/s) introduced by the nonideal behavior of the sensor is also twice the motor speed (in rad/s), since the major axis of the ellipse is travelling twice as fast as the wave generator. This makes it impossible to discern the true ripples caused by the gear meshing vibration from that caused by nonideal measurement. As illustrated in Fig. 7, the power spectrum of the measured torque plotted for the time interval 0.8 s to 1.1 s when the velocity is almost flat and about 156 rad/s shows two peaks, at 312 and 624 rad/s. This confirms the existence of the fundamental frequency of the oscillation as twice the velocity and shows the significance of the next important first-harmonic frequency of four times the velocity. The dependence of the frequency content of the torque ripples on the velocity makes it possible to model them as a simple harmonic oscillator and to employ a Kalman filter to predict and filter them from the torque measurement. If only low-frequency torque control is desired [5], the high-frequency ripples may be removed by estimating them via Kalman filtering. This is more efficient than simple low-pass filtering, because it uses the known structure of the torque signal.

A fourth-order harmonic oscillator error model can characterize both the fundamental and first-harmonic frequency content of the torque ripple. This can be represented by the following time-varying discrete state space form:

$$\begin{aligned} \boldsymbol{x}(k+1) &= \left[\begin{array}{c|c} \boldsymbol{\Phi}_1(k) & \mathbf{0} \\ \hline \mathbf{0} & \boldsymbol{\Phi}_2(k) \end{array}\right]\boldsymbol{x}(k) + \boldsymbol{w}(k) \\ y(k) &= [1\ 0\ 1\ 0]\boldsymbol{x}(k) + v(k) \end{aligned} \tag{5}$$

where

$$\boldsymbol{\Phi}_i(k) = \begin{bmatrix} \cos(\omega_i(k)T_s) & \sin(\omega_i(k)T_s) \\ -\sin(\omega_i(k)T_s) & \cos(\omega_i(k)T_s) \end{bmatrix} \tag{6}$$

in which T_s is the sampling period, and $\omega_1(k) = 2\dot{\theta}(k), \omega_2(k) = 4\dot{\theta}(k)$, and $\dot{\theta}(k)$ is the motor shaft velocity in rad/s at time step k, hence $\boldsymbol{\Phi}_i(k)$ is a time-varying matrix adapting with changes in the velocity. Moreover, y is the torque ripple, which needs to be observed from the torque measurement by having a crude model for the expected

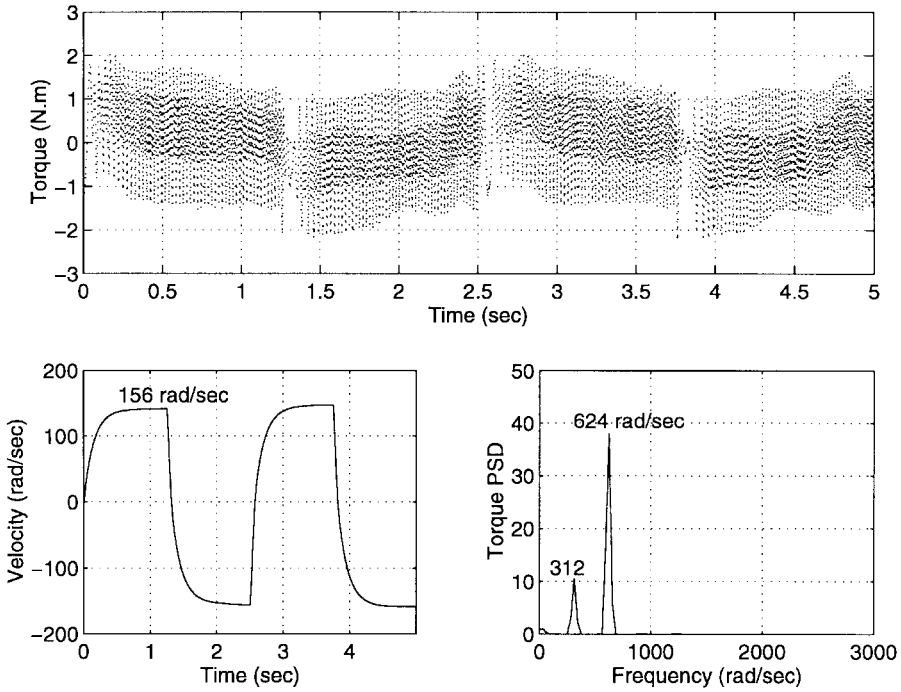

Fig. 7. Measured torque and velocity and the power spectrum of the measured torque with peaks at multiples of the velocity.

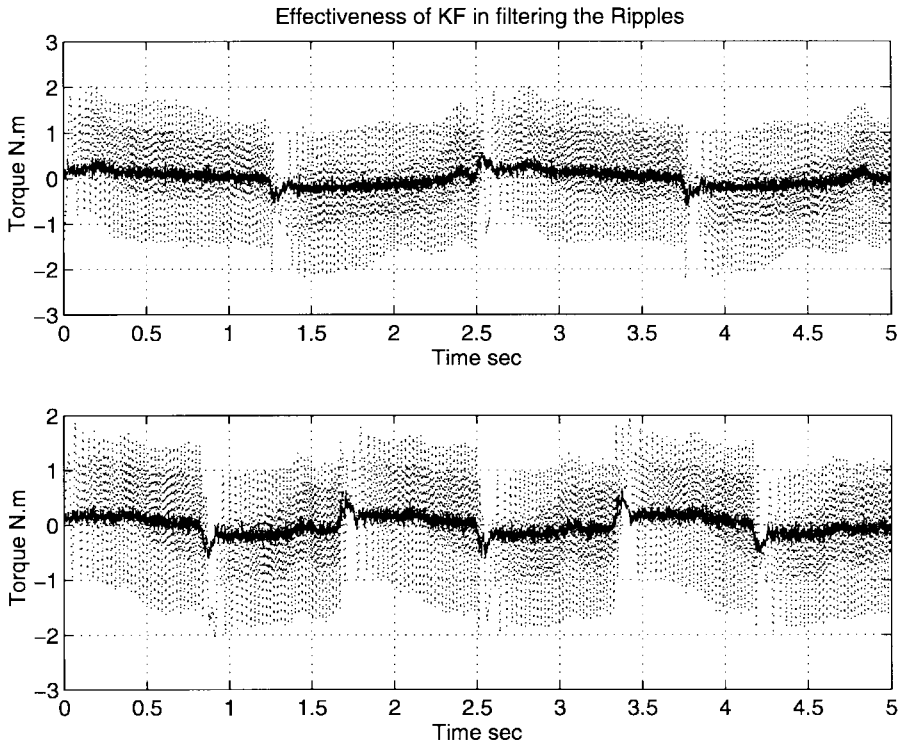

Fig. 8. Kalman filter performance to cancel torque ripples. Dotted: measured torque, solid: Kalman filtered torque.

torque. If measured torque is indicated by T_{meas} and the expected torque is indicated by T_{exp}, then torque ripple $y(k) = T_{\text{meas}}(k) - T_{\text{exp}}(k)$, while the difference between true torque and the crude estimate of the expected torque is encapsulated by the measurement errors in $v(k)$ in (5). Therefore, no accurate model for the expected torque T_{exp} is necessary, and hence, for free motion experiments, the expected torque can be estimated simply by the inertial part of the output torque which is the load inertia multiplied to the load acceleration. The first two elements of the state $\boldsymbol{x}$ consist of the component of the torque ripple due to the fundamental frequency ω_1 and its derivative, while the next two elements are those components of torque ripple due to the first-harmonic frequency ω_2 and its derivative. Therefore, the

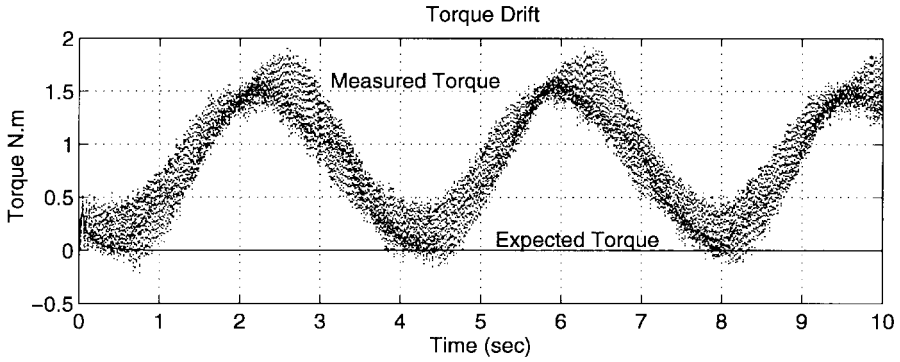

Fig. 9. Misalignment torque signature on the measured torque.

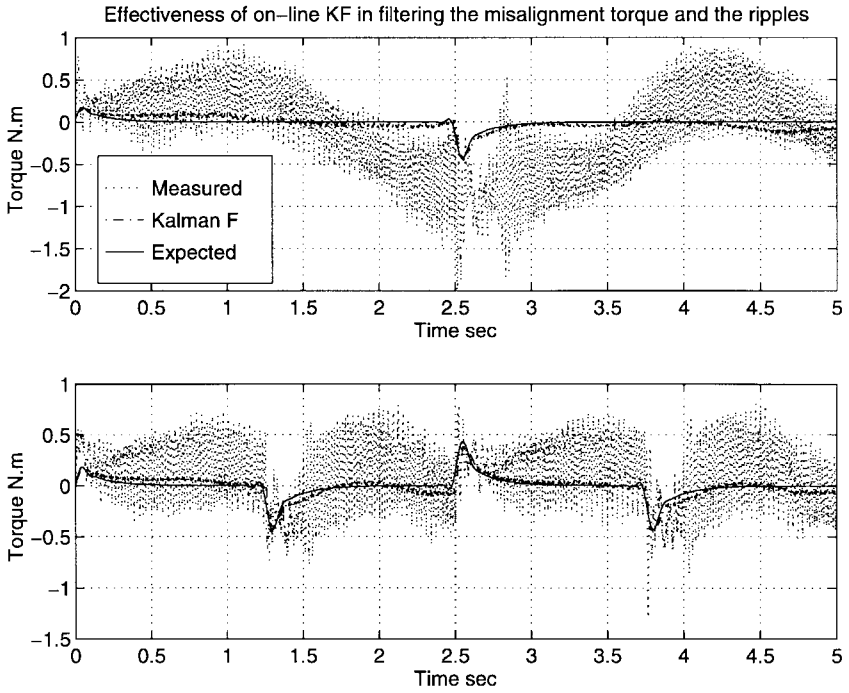

Fig. 10. Kalman filter performance to cancel torque ripples, and misalignment torque for two typical experiments.

total torque ripple is calculated by adding the first and third element of the state. $\boldsymbol{w}(k)$ characterizes the other frequency components of the torque ripples which will not be estimated in this model.

Using the fourth-order harmonic oscillator model for the torque ripples, a prediction-type time-varying Kalman filter algorithm is applied to estimate the torque ripples [14]. A prediction-type estimate is computationally faster than a current-estimate type of Kalman filter and therefore preferable for online implementation. Assuming that the process noise $\boldsymbol{w}(k)$ and measurement noise $v(k)$ are zero-mean Gaussian white and have covariances defined by $\boldsymbol{Q}$ and R as

$$E\{\boldsymbol{w}(k)\boldsymbol{w}^T(k)\} = \boldsymbol{Q}, \quad E\{v(k)v^T(k)\} = R \tag{7}$$

the states estimates is calculated using Kalman filter formulation [14] as follows:

$$\hat{\boldsymbol{x}}(k+1) = \boldsymbol{\Phi}(k)\hat{\boldsymbol{x}}(k) + \boldsymbol{K}_e(k)[\boldsymbol{y}(k) - \boldsymbol{C}(k)\hat{\boldsymbol{x}}(k)] \tag{8}$$

in which the Kalman filter gain $\boldsymbol{K}_e(k)$ will be updated from

$$\boldsymbol{K}_e(k) = \boldsymbol{\Phi}(k)\boldsymbol{P}(k)\boldsymbol{C}^T(k)[R(k) + \boldsymbol{C}(k)\boldsymbol{P}(k)]\boldsymbol{C}^T(k)]^{-1} \tag{9}$$

$$\boldsymbol{P}(k+1) = \boldsymbol{Q}(k) + [\boldsymbol{\Phi}(k) - \boldsymbol{K}_e(k)\boldsymbol{C}(k)]\boldsymbol{P}(k)\boldsymbol{\Phi}^T(k). \tag{10}$$

Since the measurement signal $y(k)$ is a scalar, its covariance matrix $R(k)$ is also a scalar, and no matrix inversion is required for online implementation of the Kalman filter gain given in (9). Fig. 8 illustrates the performance of the Kalman filter implemented on line with a sampling frequency of 1 kHz to estimate and filter the torque ripples for two typical experiments, in which $\boldsymbol{Q} = 10^3\boldsymbol{I}_{4\times4}$ and $R = 1$. The performance of the Kalman filter for torque ripple cancellation is shown to be quite fast and accurate.

V. Misalignment Torque Compensation

The Kalman filter can be used not only to estimate the torque ripples, but also to cancel any mechanical misalignment torque

signature on the measured torque. Many torque sensors exhibit the limitation of being sensitive to the torques applied on the direction perpendicular to their axis of measurement. In our setup, after repeated use of the harmonic drive system for different experiments, a similar torque signature was observed on the measured torque. Fig. 9 illustrates a simple experiment in which the harmonic drive is driven by a constant velocity but the measured torque exhibits a sinusoidal trend. The expected torque, the solid line in Fig. 9, is constant after a short time of acceleration, but the measured torque, dotted lines, displays a sinusoidal behavior. After examining the system accurately, the source of this torque signature is found to be the misalignment of the harmonic drive shaft and the load. By disassembling the system and carefully reassembling it, the peak-to-peak amplitude of this misalignment signature was reduced from 10 N $\cdot$ m to less than 2 N $\cdot$ m. However, in practice it is quite expensive, and probably infeasible to perfectly align all the moving components. Fortunately, the sinusoidal feature of this misalignment torque makes it possible to accurately estimate them with an error model. The frequency of misalignment torque (in rad/s), as it can be intuitively identified from its source of generation, is exactly the same as the output shaft velocity (in rad/s). Therefore, adding another block to the harmonic oscillator model [given in (5)] of the system with frequency $\omega_3(k) = vel(k)/$(Gear Ratio), will estimate the misalignment component of the measured torque. Using this sixth-order model for the torque ripple and misalignment torque together, Fig. 10 illustrates the Kalman filter performance in cancelling those elements for two typical experiments. The Kalman filtered torque is shown to cancel the torque ripples and misalignment torque quite accurately. These results are obtained using an online Kalman filter implementation on the system with sampling frequency of 1 kHz. Contrary to low-pass filtering which is incapable of extracting the misalignment torque from the measurements, Kalman filter estimation proved to be fast and accurate to filter both torque ripples and misalignment torque. Moreover, it is a reliable method for different operating ranges, and therefore, preferable for torque feedback.

VI. Conclusions

In this paper the built-in torque sensor for harmonic drive systems as first proposed by Hashimoto is examined in detail. By this method, strain gauges are directly mounted on the flexspline, and therefore, no extra flexible element is introduced into the system. To have minimum sensing inaccuracy, four Rosette strain gauges are employed using an accurate method of positioning. An accurate drawing of the strain gauge placement positions is printed on a transparent film, and the strain gauges are placed on the transparent film using a microscope. Then the transparent film is accurately placed on the flexspline, and the strain gauges are cemented on the surface. It is shown that employing this method reduces the positioning error to a minimum. Calibration of the torque sensor shows that the sensor is performing linearly and the torque readings are not dependent on the position of the flexspline.

One important characteristic of harmonic drive torque transmission, as observed in free motion experiments, is a high frequency oscillation in the output torque signal. To cancel these oscillation, named torque ripples, from the measured torque, Kalman filter estimation is employed. Due to the dependence of the frequency content of the torque ripples on the wave generator velocity, a simple fourth-order harmonic oscillator proved to accurately model the torque ripples. The performance of Kalman filter to cancel the torque ripples from torque measurements is shown to be very fast and accurate. Moreover, the error model is extended to incorporate any misalignment torque signature. By on-line implementation of the Kalman filter incorporating a sixth-order model, it is shown that this method is a fast and accurate way to filter torque ripples and misalignment torque, and hence, this intelligent built-in torque sensor is preferable for torque feedback.

References

[1] H. D. Taghirad and P. R. Bélanger, "An experimental study on modeling and identification of harmonic drive systems," in *Proc. IEEE Conf. Decision and Control*, vol. 4, Dec. 1996, pp. 4725–4730.

[2] S. Nicosia and P. Tomei, "On the feedback linearization of robots with elastic joints," in *Proc. IEEE Conf. Decision and Control*, vol. 1, 1988, pp. 180–185.

[3] M. W. Spong, J. Y. Hung, S. Bortoff, and F. Ghorbel, "Comparison of feedback linearization and singular perturbation techniques for the control of flexible joint robots," in *Proc. American Control Conf.*, vol. 1, 1989, pp. 25–30.

[4] M. W. Spong, "Adaptive control of flexible joint manipulators," *Syst. Contr. Lett.*, vol. 13, no. 1, pp. 15–21, July 1989.

[5] H. D. Taghirad and P. R. Bélanger, "Intelligent torque sensing and robust torque control of harmonic drive under free-motion," in *Proc. IEEE Int. Conf. Robotics and Automation*, vol. 2, Apr. 1997, pp. 1749–1754.

[6] R. Hui, N. Kircanski, A. Goldenberg, C. Zhou, P. Kuzan, J. Weircienski, D. Gershon, and P. Sinha, "Design of the iris facility—a modular, reconfigurable and expandable robot test bed," in *Proc. IEEE Int. Conf. Robotics and Automation*, vol. 1, 1993, pp. 155–160.

[7] D. Stokic and M. Vukobratovic, "Historical perspectives and state of the art in joint force sensory feedback control of manipulation robots," *Robotica*, vol. 11, no. 2, pp. 149–157, Mar./Apr. 1993.

[8] M. Hashimoto, "Robot motion control based on joint torque sensing," in *Proc. IEEE Int. Conf. Robotics and Automation*, 1989, pp. 256–261.

[9] M. Hashimoto, Y. Kiyosawa, H. Hirabayashi, and R. P. Paul, "A joint torque sensing technique for robots with harmonic drives," in *Proc. IEEE Int. Conf. Robotics and Automation*, vol. 2, Apr. 1991, pp. 1034–1039.

[10] H. D. Taghirad and P. R. Bélanger, "Robust torque control of harmonic drive under constrained motion," in *Proc. IEEE Int. Conf. Robotics and Automation*, vol. 1, Apr. 1997, pp. 248–253.

[11] M. Hashimoto, Y. Kiyosawa, and R. P. Paul, "A torque sensing technique for robots with harmonic drives," *IEEE Trans. Robot. Automat.*, vol. 9, no. 1, pp. 108–116, Feb. 1993.

[12] H. D. Taghirad, P. R. Bélanger, and A. Helmy. An experimental study on harmonic drive. Technical Report submitted to the International Submarine Engineered Ltd., Port Coquitlam, B.C., Canada, http://www.cim.mcgill.ca/$^{-}$taghirad, 1996.

[13] I. Godler, K. Ohnishi, and T. Yamashita, "Repetitive control to reduce speed ripple caused by strain wave gearing," *IECON Proc.*, vol. 2, pp. 1034–1038, 1994.

[14] K. Ogata, *Discrete-Time Control Systems.* Englewood Cliffs, NJ: Prentice-Hall, 1995.

Hamid D. Taghirad, photograph and biography not available at the time of publication.

P. R. Bélanger, photograph and biography not available at the time of publication.